UDK 669.058.6:658.5
Original scientific article/Izvirni znanstveni članek

ISSN 1580-2949
Mater. Tehnol.

ENHANCED SURFACE ENGINEERING OF ENB ALLOY COATINGS: TRIBO-MECHANICAL INSIGHTS INTO HEAT TREATMENT AND SODIUM BOROHYDRIDE LEVELS

NAPREDNI INŽENIRING POVRŠIN ENB PREVLEK: TRIBO-MEHANSKI VPOGLED V TOPLOTNO OBDELAVO IN NATRIJ-BOR HIDRIDNIH NIVOJEV

D. R. P. Rajarathnam[1*], S. Senthil Babu[2], Fatima Firdous Nikhat[3], M. Selvaraj[4], R. T. Ajaykarthik[5]

[1]Paavai Engineering College, Department of Mechatronics Engineering, Namakkal, India
[2]SRMIST, Department of Mechanical Engineering, Ramapuram, Chennai, India
[3]Khaja Bandanawaz University, Department of Mechanical Engineering, Kalaburagi, India
[4]Paavai Engineering College, Department of Mechanical Engineering, Namakkal, India
[5]Paavai Engineering College, Department of Mechatronics Engineering, Namakkal, India

Prejem rokopisa – received: 2025-05-29; sprejem za objavo – accepted for publication: 2025-08-21

doi:10.17222/mit.2025.1469

The optimization of coating parameters was the main focus of earlier research on electroless Ni-B (ENB) coatings; nevertheless, little is known about how bath composition and heat treatment temperature affect nanoindentation characteristics such scratch hardness, elastic modulus, and nanohardness. EN8 steel specimens with different concentrations of sodium borohydride ($NaBH_4$) are coated with ENB and heated at (355, 455 and 555) °C in order to examine these aspects. The results show that a higher boron content and larger nodules, raising the concentration of $NaBH_4$, improve nanohardness and elastic modulus. Due to the production of boride phases, which contribute to a more compact shape, these qualities are further enhanced with heat treatment. Additionally, scratch hardness rises with the concentration of $NaBH_4$, peaking at 455 °C, where the hard Ni_2B phase is most noticeable. Due to their homogenous and compact structure, the coatings show better resistance to wear and friction, even when their surface roughness decreases after being heated.

Keywords: optimization, bath composition, elastic modulus, friction resistance, nodules

V predhodnih raziskavah so se raziskovalci osredotočali predvsem na optimizacijo parametrov izdelave prevlek z brez-električnim postopkom izdelave Ni-B (ENB) prevlek. Malo pa je bilo do sedaj znanega o sestavah kopeli in vplivu temperature toplotne obdelave na nano-trdoto, karakteristike razenja in elastični modul. Da bi osvetlili še ta aspekt so avtorji v predstavljeni študiji vzorce podlage iz EN8 jekla prevlekli z ENB postopkom in pri tem uporabili različne koncentracije natrij-borhidrida ($NaBH_4$) ter različne temperature termične obdelave (355 °C, 455 °C in 555 °C). Rezultati raziskave so pokazali, da se zaradi višje vsebnosti bora v prevlekah (višje koncentracije $NaBH_4$) izboljšata nanotrdota in modul elastičnosti. Zaradi tvorbe boridnih faz, ki prispevajo k bolj kompaktni obliki, toplotna obdelava še dodatno prispeva k izboljšanju lastnosti prevlek. Testi razenja prevlek pa so pokazali, da se s povečevanjem koncentracije $NaBH_4$ pri 455°C najbolj občutno pokaže vpliv NixB faze na trdoto prevleke oziroma njeno odpornosti proti razenju. Zaradi homogene in kompaktne strukture imajo prevleke boljšo odpornost proti obrabi in manjši koeficient trenje, celo ko se njihova površinska hrapavost slabša zaradi ogrevanja.

Ključne besede: optimizacija, sestava kopeli, elastični modul, upor zaradi trenja, nodule

1 INTRODUCTION

The increased tribological qualities of electroless Ni-B (ENB) alloy coatings are well recognized, mostly due to their characteristic cauliflower-like surface form, which reduces the real contact area and improves frictional behavior.[1,2] When these coatings are applied to mild steel substrates, they also help to raise the surface hardness.[3,4] Numerous investigations examined ENB coatings considering factors such tribological behavior, surface morphology, hardness, roughness, plating rate, and coating thickness.[3,4] The composition of ENB coatings was found to have a substantial impact on their qualities; this composition is dependent on temperature, pH, and bath content. The boron content of the coating films is highly sensitive to the temperature of bath[3–4] and concentration of $NaBH_4$.[3,5] Even small variations in these factors can influence the coating's phase structure, surface morphology, and overall characteristics.

As the quantity of boron increases, so does the phase structure of ENB coatings. At intermediate boron levels, the coatings change from a crystalline structure at low boron concentrations to a mixture of crystalline and amorphous phases.[3,5] The structure mostly takes on an amorphous form as the boron level rises.[3] Phase changes in ENB coatings are said to start at about 300 °C,[6,8] where heat treatment causes crystalline phases like Ni,

*Corresponding author's e-mail:
drprajamalathi@yahoo.co.in (D. R. P. Rajarathnam)

Ni_2B, and Ni_3B to develop.[6,7] Compared to their amorphous counterparts, coatings with a crystalline structure have shown better corrosion resistance.[3] A compact and uniform surface shape is probably the reason why hardness and wear resistance increase as boron content rises.[3] Heat treatment enhances these properties[9] by promoting the formation of hard phases such as Ni_2B and Ni_3B.[6,10] Significantly, hardness rises sharply at a 6 % boron concentration threshold but is largely constant above it.[11] Moreover, hardness increases with prolonged heat treatment, peaking at about 455 °C as a result of the development of hard boride phases.[12]

By adding hard particles like Mo and W, the performance of binary alloy coatings can be further improved.[10,13,14] When nano- or micro-sized particles are added to a metal matrix, the properties of the coating are changed. For example, nickel-based binary and ternary coatings use nanoparticles such as ZrO_2 and Al_2O_3 to enhance the surface hardness and Young's modulus, refining the grain structure.[15] The incorporation of nanoparticles such as TiO_2 and nanodiamonds (ND) into an Ni-B matrix was shown to improve its hardness, corrosion resistance, and wear properties.[16]

The chemical makeup, phase structure, and surface morphology of ENB coatings are all significantly influenced by the bath composition and operation circumstances. These parameters also affect phase transitions, morphology, and plating rate. Prior research employed nanoindentation techniques to assess the mechanical behavior of ENB coatings at specified bath concentrations. The influence of variations in the heat treatment temperature and the concentration of the reducing agent on scratch hardness, elastic modulus, and nanohardness remains largely unexplored. In order to close this gap, ENB coatings with varying concentrations of $NaBH_4$ were deposited and then heat-treated at varied temperatures. The variations in scratch hardness, elastic modulus, and nanohardness were correlated with the resulting transformations in the phase structure and surface morphology.

2 EXPERIMENTAL METHODOLOGY

2.1 Deposition process for coatings

ENB coatings were deposited onto EN8 steel substrates. The substrates were mostly composed of 0.68–0.85 weight percent Mn, 0.03 *w*/% S, 0.06 *w*/% P, 0.32–0.43 *w*/% C, and 0.10–0.25 *w*/% Si, with the remaining percentage being Fe. For the examination of mechanical properties, square specimens measuring (20 × 20 × 3) mm were made, and for friction and wear testing, cylindrical samples measuring Ø8 × 35 mm were utilized. After first being cleaned and smoothed with soap water, the specimens were rinsed with acetone to get rid of any remaining oil. The rust and oxide coatings were removed by treating them with a 50 % HCl solution. The flawless specimens were washed and then submerged in a chemical solution to deposit the coating. A steel surface is catalytically active for deposition, thus a second pre-treatment in a lukewarm $PdCl_2$ solution was used to expedite the process.

The coating deposition process was carried out in a 200 mL bath with a bath load maintained between 29.5 cm^2/L and 32.1. In this investigation, bath replenishment was used to maintain the bath stability and deposition efficiency rather than mechanical or ultrasonic agitation. After two hours, the bath solution was changed to avoid a diffused layer forming as a result of the reactive species being depleted. Four hours was the set amount of time for the deposition process. The concentrations of $NiCl_2$ (20 g/L) and $NaBH_4$ (0.60, 0.90, and 1.20) g/L in the coating bath were classified as low, medium, and high for the nickel and boron sources, respectively. The buffer was NaOH (40 g/L), and the complexing agent was $C_2H_8N_2$ (59 g/L). We added $PbNO_3$ (0.0145 g/L) as the stabilizer. A pH of 12.5 and a bath temperature of 95 ± 2 °C were maintained. After being coated, the specimens were heated for one hour at 355 °C (HT355), 455 °C (HT455), and 555 °C (HT555) before being cooled within the furnace.

2.2 Properties of the coating

A secondary electron detector-equipped scanning electron microscope (HITACHI SU3800, Japan) was used to examine the ENB coating surface morphology. Energy-dispersive X-ray analysis operating at 10–15 keV was used to determine the elemental composition of the material. Low-energy X-rays were transmitted through a super-thin window. A silicon (Si) standard was used to calibrate the EDAX system. Comparing a typical boron sample spectrum to the untreated coating spectrum allowed us to determine the coating's boron concentration.[7,17] Cu-Kα radiation was used for the XRD analysis, spanning over a diffraction angle range (2θ) of 20–90° at a scanning speed of 0.02° per second.

2.3 Measurement of wear and friction

The wear and friction characteristics of the coated specimens were evaluated using a pin-on-disc multi-capacity tribotester (Model: POD 4.0, DUCOM, India) in dry sliding conditions. The tests were conducted in compliance with ASTM G99-05 (Reapproved in 2010) requirements. For the tribological evaluation, cylindrical specimens with a diameter of Ø8 mm and a length of 35 mm were utilized. The revolving disc was composed of EN31 steel (58-68 HRC), measuring 11.5 cm in diameter and 8 mm in thickness. The specimens were forced up against the rotating disk and subjected to a standard load of 50 N during the testing process. The track diameter was 6 cm, the entire sliding distance was 471 m, and the slip velocity was kept at 0.4010 m/s. A computer-integrated data acquisition system was utilized to measure the frictional force at the interface where the rotating

disc comes into contact with the coated specimen. A precision weighing balance with an accuracy of 0.01 mg was used to measure the mass of each specimen both before and after testing. Using the formula provided, which is based on the mass loss seen during these observations, the precise wear rate was calculated.

$$W_s = M/S \times P \quad (1)$$

where M signifies the amount of material loss (kg), S represents the total distance covered (m), and P indicates the applied load (N).

2.4 Load-bearing properties

A triangular pyramidal diamond-tipped Berkovich indenter was connected to a nanoindentation test apparatus (Nano Indenter® G200 by Labindia Instruments, India) to conduct nanoindentation testing. 500 nm was the greatest depth of indentation.[12] The rate of loading and unloading remained steady at 40 mN per minute, with a pause of two seconds between two processes. The Oliver and Pharr technique was utilized to determine both the hardness and Young's modulus.[12] To lessen the substrate's influence on the results, the indentation depth was kept below a minimum coating thickness of 1/10th.[6] To reduce the impact of surface roughness, the coated samples were polished using an ultra-fine diamond paste before testing. Each sample was measured at ten points along a line, and the tests were conducted on three samples produced from an identical bath mixture. The mean values of different measurements were recorded.

Micro-scratch test equipment (Model: BGS 520 Automatic Scratch Tester, Make: CALTECH, India) was used to assess the scratch hardness in compliance with ASTM G171-03 standard. In the testing setup, a 200 µm Rockwell C-type diamond tip radius indenter was used. The experiments were conducted with a consistent scratch speed of 0.1 mm/sec over a scratch length of 5 mm, while applying a load of 20 N. The scratch width was measured 10 times, and the following formula was used to calculate the scratch hardness based on the average value:

$$HS_P = 24.98\ N/Y^2\ (\text{GPA}) \quad (2)$$

HS_P signifies the scratch hardness, N represents the applied load measured in grams, and Y corresponds to the scratch width expressed in micrometers.

3 ANALYSIS OF RESULTS

3.1 Coating characterization

Equivalent images obtained with a SEM analysis of the ENB samples' cross-sectional thickness are shown in **Figure 1**. At low concentrations of $NaBH_4$, the minimum coating thickness is 13 µm.[3] For medium and high doses of $NaBH_4$, the thickness values are 27.89 µm and 30.69 µm, respectively. An increase in the $NaBH_4$ con-

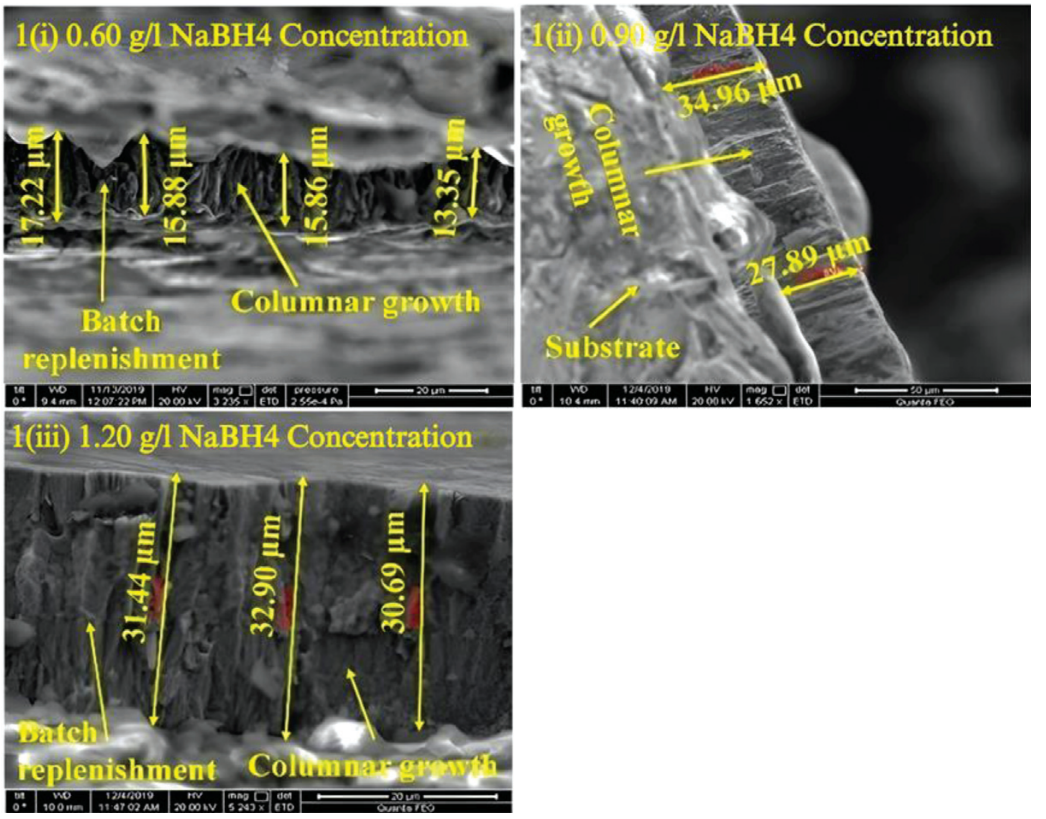

Figure 1: Cross-sectional SEM pictures depict the thickness of untreated ENB coatings formed at varying $NaBH_4$ concentrations: (i) 0.60 g/L; (ii) 0.90 g/L; and (iii) 1.20 g/L

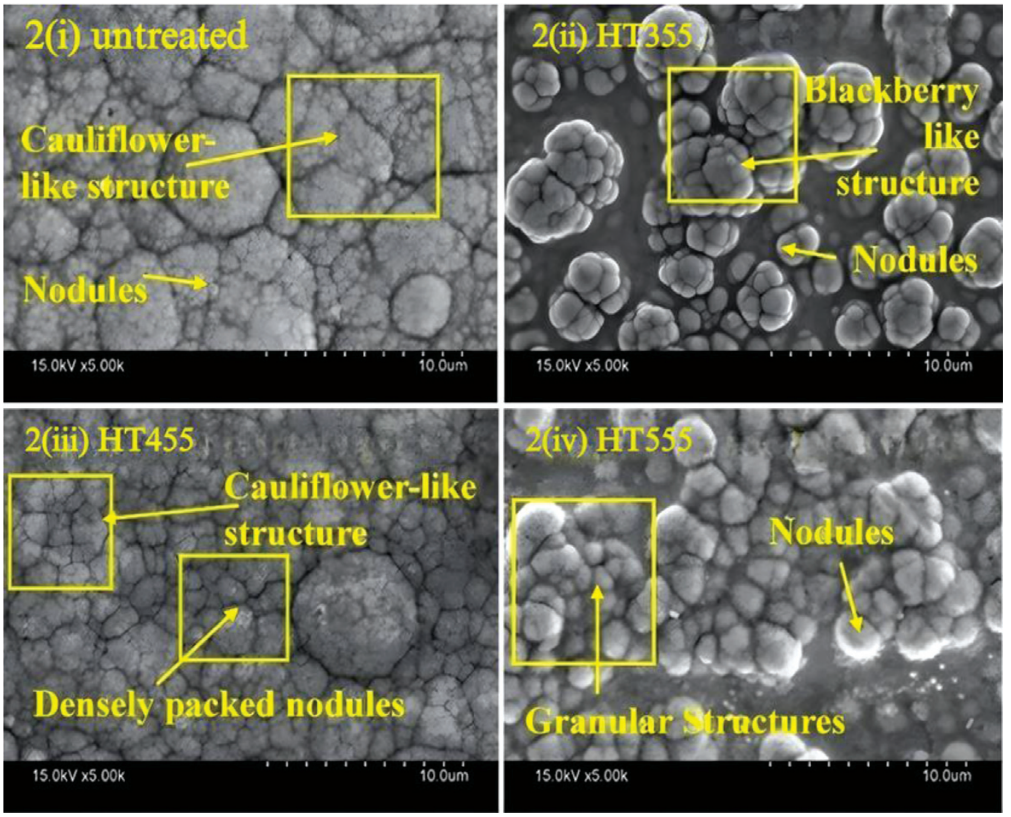

Figure 2: SEM pictures of electroless Ni-B coating with 0.60 g/L of $NaBH_4$, captured under different conditions: (i) untreated; (ii) HT355; (iii) HT455; (iv) HT555

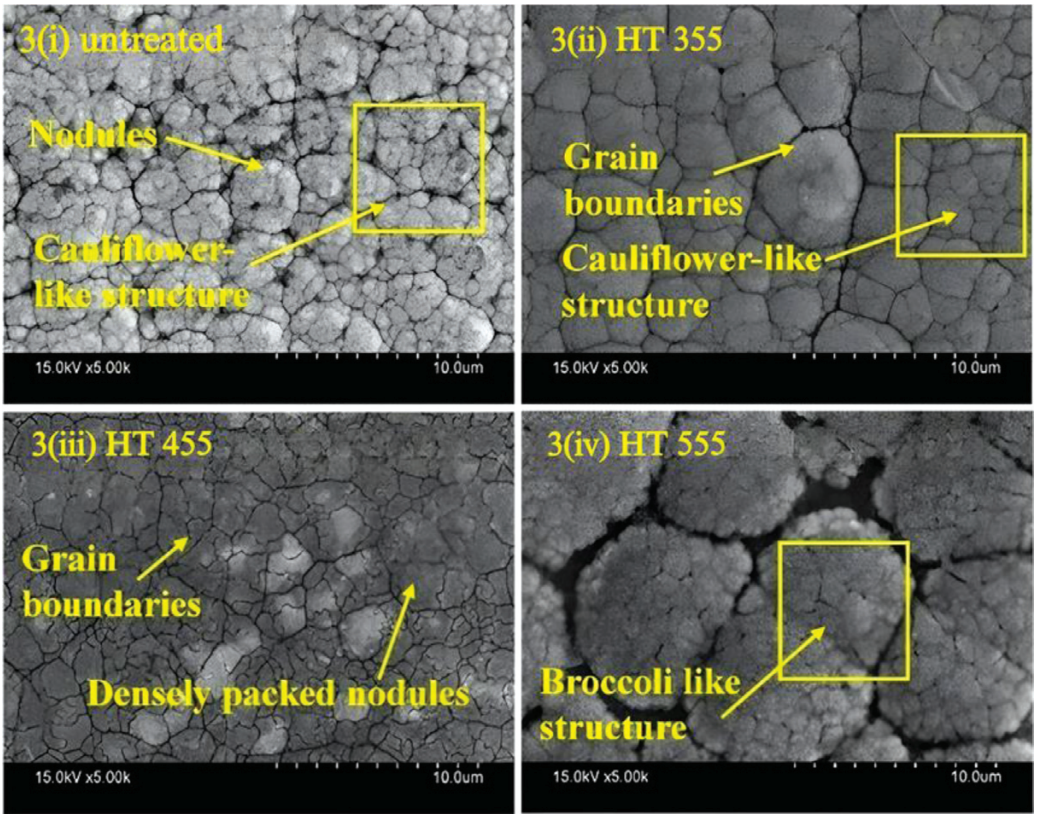

Figure 3: SEM pictures of electroless Ni-B coating with 0.90 g/L of $NaBH_4$, captured under different conditions: (i) untreated; (ii) HT355; (iii) HT455; (iv) HT555

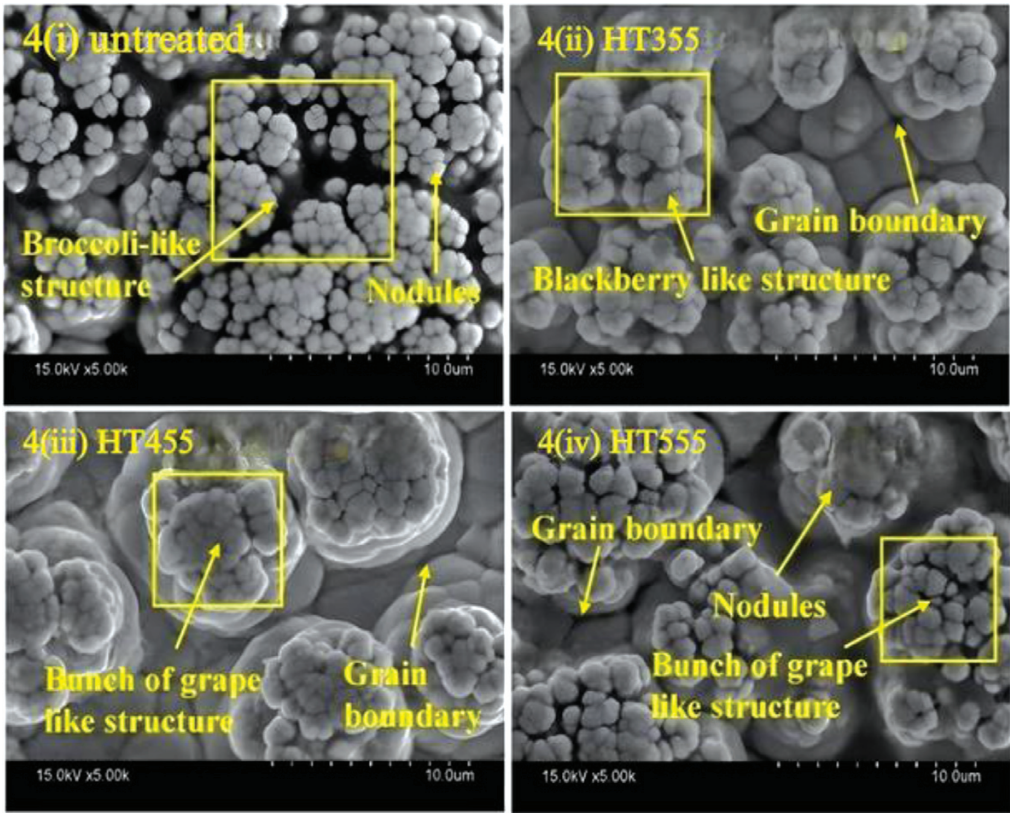

Figure 4: SEM pictures of electroless Ni-B coating with 1.20 g/L of $NaBH_4$, captured under different conditions: (i) untreated; (ii) HT355; (iii) HT455; (iv) HT555

centration leads to a corresponding growth in the coating thickness. To obtain reliable results, each sample is deposited for four hours. A higher $NaBH_4$ concentration accelerates the rate of reduction, which accelerates the rate of deposition and thickens the coating. The coating thicknesses for borohydride concentrations of 0.60–1 g/L ranged from 9 μm to 22 μm, in line with the earlier study, which showed a similar tendency.[4]

Low, medium, and high concentrations of $NaBH_4$ resulted in coatings with boron contents of (3.5±0.40, 6.60±0.50 and 8.70±0.40) %, respectively. The concentration of $NaBH_4$ and boron content are directly correlated, which is in line with the earlier study.[7] A greater boron incorporation in the coating layers is the result of an improved reduction reaction made possible by higher $NaBH_4$ levels. The boron content of the coatings with a medium $NaBH_4$ concentration is 6.5–7 %, which is consistent with previous findings.[18]

In **Figures 2–4**, the examination of the surface characteristics of ENB coatings is presented. A homogeneous surface morphology and an even distribution of nodules throughout the studied area are revealed by the SEM images of the untreated specimens, displayed in **Figures 2i**, **3i**, and **4i** show the coatings in their untreated condition, exhibiting a surface morphology resembling cauliflowers or broccoli.[1,2] The nodules are larger and more pronounced at higher doses of $NaBH_4$, giving them a broccoli-like appearance (**Figure 4i**). This structure is usually made up of tiny grains.[19] **Figures 2i**, **2iii**, **3i**, and **3iii** show that even after heat treatment, the coatings maintain their cauliflower-like appearance.

Starting at the metal surface, the deposition process moves vertically, producing columnar growth, which predominates over horizontal expansion.[14] As illustrated in **Figure 1**, this columnar growth aids in the development of a cauliflower-like shape. The transformation from a cauliflower-like morphology to a nodular structure is attributed to grain interaction and fusion, leading to formations resembling blackberries or grape clusters.[19] This structural evolution is evident in **Figures 2ii**, **2iv**, **3iv**, **4ii**, **4iii**, and **4iv**. Due to improved grain contact, the coatings acquire a nodular surface shape when the concentration of $NaBH_4$ increases and heat treatment is applied.[19] There are clear grain boundaries and a compact morphology in Figure 3iii. Localized fusion causes some noticeable grain boundaries to become visible, even if the grains combine to produce a dense structure.

X-ray diffraction (XRD) patterns of the ENB coatings are displayed in **Figure 5**. There is a hump in the untreated condition and a noticeable broad peak is observed at 53° for the coatings with a low concentration of $NaBH_4$.[11] This implies the existence of both nanocrystalline and amorphous phases.[1,10,11] In the untreated state, the XRD pattern exhibits a broad hump, indicating the presence of predominantly amorphous and nanocrystalline phases. Upon heat treatment at 355 °C, the

onset of crystallization occurs with the emergence of minor Ni and Ni_3B phases. Further heating to 455 °C results in the appearance of clear and sharp peaks of Ni_2B, corresponding to the maximum hardness and enhanced scratch resistance of the coating. However, at 555 °C, the intensity of Ni_2B peaks diminishes, while Ni_3B phases become more dominant, leading to a slight reduction in hardness. During heating, boron atoms initially diffuse into the nickel lattice, resulting in the formation of a Ni–B solid solution. With further increase in thermal activation, the excess boron atoms tend to segregate, promoting the nucleation of Ni_2B at around 455 °C. As the temperature increases further to approximately 555 °C, the thermodynamic stability shifts, leading to the transformation and growth of Ni_3B phases. This sequence highlights the progressive evolution from the solid solution to stable boride phases under varying heat treatment conditions. In general, the coatings that contain less than 4.3 % boron have an amorphous structure.[8,20] On the other hand, the coatings created with medium and high concentrations of $NaBH_4$ only show one hump in their untreated state,[1,8,11] suggesting a more noticeable amorphous character. A structural shift to an amorphous phase is shown by the lack of a broad crystallinity peak when the boron content rises with increasing $NaBH_4$ concentrations.[3,4]

3.2 Mechanical properties

ENB coatings increase the hardness of steel, as shown in **Table 1**, summarizing the nanoindentation test results. In the untreated state, higher concentrations of $NaBH_4$ increase the hardness and elastic modulus. The boron content impacts the coating hardness, with higher $NaBH_4$ concentrations resulting in higher hardness. With the $NaBH_4$ concentration, nanohardness also increases; however, it stays relatively steady until the medium level. This study's medium boron content of roughly 6.6 % places these coatings under the category of mid-boron content. The results fit nicely with earlier research. As different hard crystalline phases precipitate after heat treatment, nanohardness improves across the working range. When low $NaBH_4$ coatings are heated to 455 °C, the Ni_2B phase, distinguished by its compact structure, forms and yields the maximum hardness value. However, at an elevated temperature of 555 °C, the Ni_2B phase is no longer present, leading to a slight reduction in hardness.

On the other hand, medium and high $NaBH_4$ coatings continue to get harder after heat treatment, most likely as a result of the additional crystalline phases that were found in previous research. Additionally, coatings with boron contents below 4.5 % have been seen to not fully crystallize, which could account for the reduced hardness

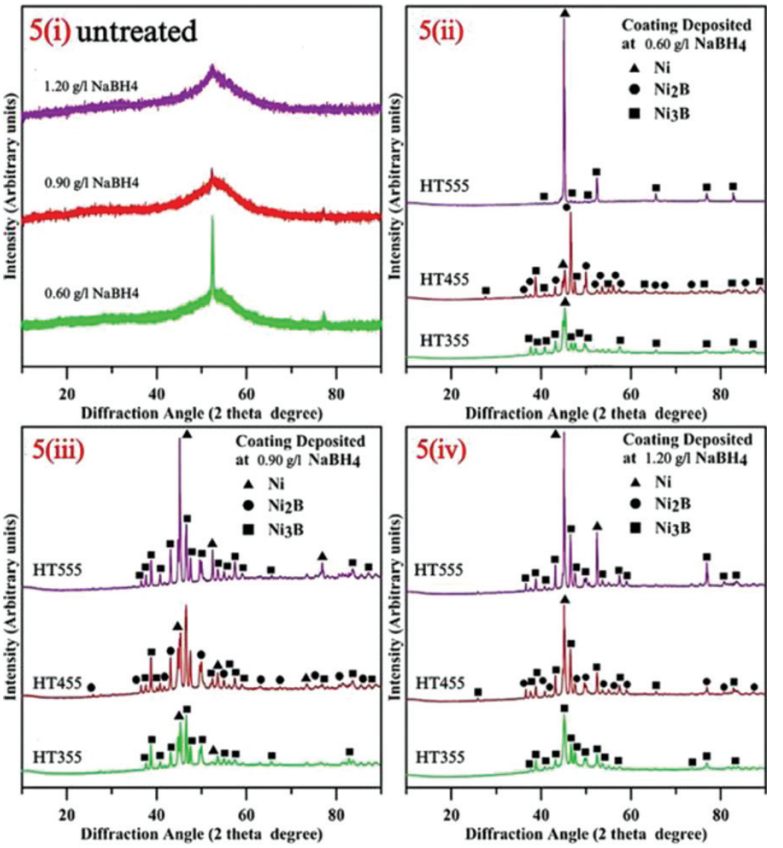

Figure 5: X-ray diffraction patterns of electroless Ni-B coating: (i) untreated; (ii) heat-treated with 0.60 g/L $NaBH_4$; (iii) heat-treated with 0.90 g/L $NaBH_4$; (iv) heat-treated with 1.20 g/L $NaBH_4$

seen at low heat-treatment temperatures and low $NaBH_4$ concentrations. Due to hard crystalline phases and the increased boron concentration, medium and high $NaBH_4$ coatings become harder after heat treatment up to 555 °C.

The increase in the elastic modulus of the untreated ENB coatings with greater concentrations of $NaBH_4$ can be linked to the relationship between elastic modulus and particle size since larger grains tend to enhance the elastic modulus.[23] Both the heat treatment duration and temperature affect these coatings' elastic modulus. Grain size expansion with extended heat treatment was reported in previous investigations, and **Table 1** demonstrates a rising trend in the elastic modulus with higher heat treatment temperatures. The enhancement of elastic modulus at elevated temperatures is likely attributed to the growth in the particle size. In accordance with earlier studies, the development of different crystalline phases also plays a role in this surge. The elastic modulus of heat-treated coatings appears to be enhanced due to the grain growth and the formation of boride phases.

For the untreated condition, the computed scratch hardness values are shown in **Table 1**, indicating an improvement with increasing $NaBH_4$ concentration. Like in the case of nanohardness, this rise in scratch hardness can be explained with the coatings' increased boron concentration. The highest scratch hardness is recorded at 455 °C, most likely as a result of the Ni_2B phase precipitating at this temperature, which increases the hardness of heat-treated coatings.[12] Values for nanohardness show a comparable pattern.

When heat treatment is applied at 455 °C, both the nanohardness and the scratch hardness of the crystalline phases, including Ni and Ni_3B, are higher than in their untreated state.[9] At 555 °C, however, the scratch hardness decreases, presumably as a result of a less compact Ni_3B phase forming in place of Ni_3B. The existence of a clustered surface morphology with clear grain boundaries may further contribute to the decrease in the scratch hardness.

The coatings analysed in this study exhibit lower scratch hardness compared to untreated Ni-B-W coatings.[14] Adding tungsten to the Ni-B matrix is known to increase hardness by strengthening the solid solution.[14] Even though the current study shows that heat treatment increases scratch hardness by precipitating crystalline phases and forming a dense coating structure, the values are still lower than those of the as-deposited Ni-B-W specimens.[14]

The strain hardening effects in the coatings are linked to the rise in scratch hardness.[14] According to the earlier study by Nemane and Chatterjee,[14] strain hardening enhances scratch resistance in multi-pass scratch testing. The heat-treated ENB coatings may have had reduced scratch hardness values as a result of the single-pass scratch test used in this investigation.

3.3 Tribological behaviour

Table 1 displays the ENB coatings' coefficient of friction (COF) values. As the concentration of $NaBH_4$ rises, the coated specimen's coefficient of friction (COF) falls. It is commonly known that surfaces that resemble cauliflowers lessen friction between surfaces that come into contact with one another. An increased nodule size and the formation of a cauliflower-like surface structure may be the cause of the decrease in COF values with increased $NaBH_4$ concentrations.[3,4] A lower COF value results from improved lubrication caused by larger nodules with such surface characteristics.[3,4] A rougher coated surface is another effect of a sharp drop in COF with rising $NaBH_4$ concentration.[1,24] Nevertheless, the COF value keeps declining at high concentrations of $NaBH_4$.[24] The tendency of surface asperities to break into debris, filling roughness valleys, smoothing the surface, and reducing the average COF, explains this occurrence.[24]

Table 1: Friction and wear performance

Parameters	Vickers hardness (*Hv*)	Young's modulus (*E*) in GPa	Scratch hardness (*HSp*) in GPa	COF	Specific wear rate (*Ws*) in x 10^{-8} kg/N.m
Nickel-boron (Ni-B) coatings with a $NaBH_4$ concentration of 0.60 g/L					
As-deposited	390	83.70	0.90	0.55	24
HT 355°C	850	125	3.65	0.70	46.95
HT 455°C	1190	147	3.65	0.66	106.72
HT 555°C	1084	154	2.78	0.60	99.69
Nickel-boron (Ni-B) coatings with a $NaBH_4$ concentration of 0.90 g/L					
As-deposited	459.28	94.40	2.70	0.35	36
HT 355°C	996	135	3.76	0.78	34.90
HT 455°C	1158	180	4.46	0.76	20.60
HT 555°C	1210	200	3.50	0.80	11.18
Nickel-boron (Ni-B) coatings with a $NaBH_4$ concentration of 1.20 g/L					
As-deposited	868.80	122.80	3.75	0.26	84
HT 355°C	1034	145	4.95	0.75	16.64
HT 455°C	1255	205	7.35	0.77	18.89
HT 555°C	1395	220	4.66	0.65	40.90

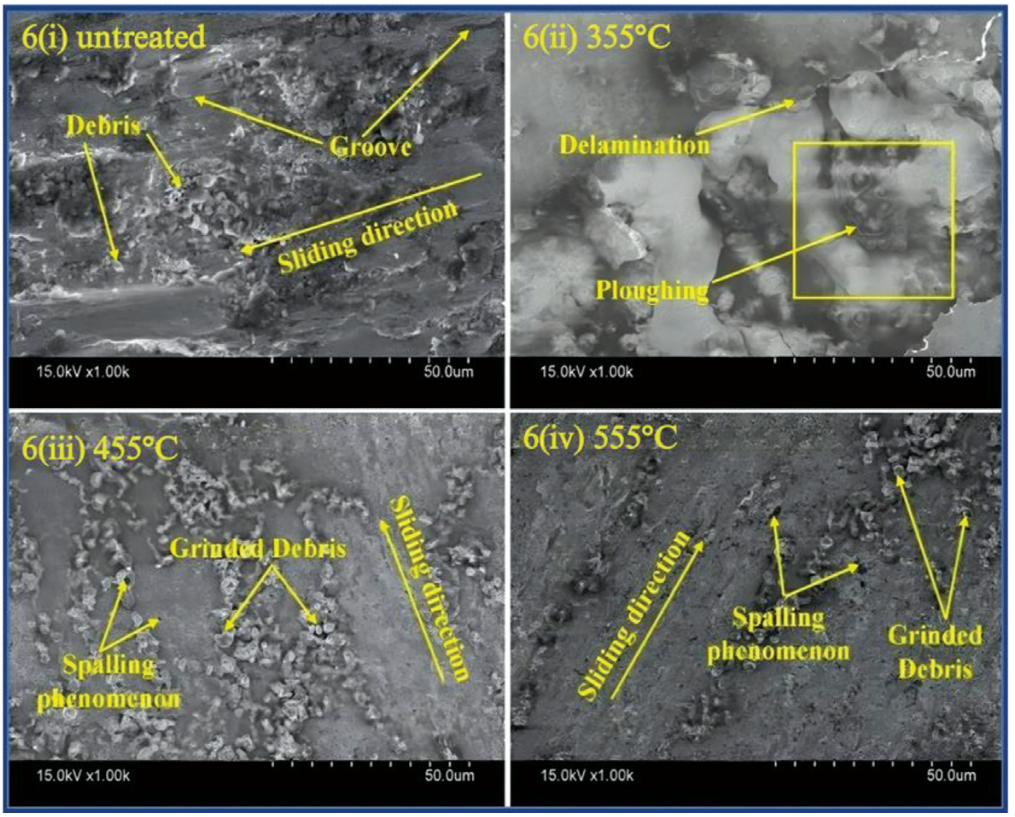

Figure 6: SEM pictures illustrating the worn surface morphologies of ENB coatings with a $NaBH_4$ concentration of 0.60 g/L in the following conditions: (i) the untreated state; after heat treatment at (ii) 355 °C; (iii) 455 °C; (iv) 555

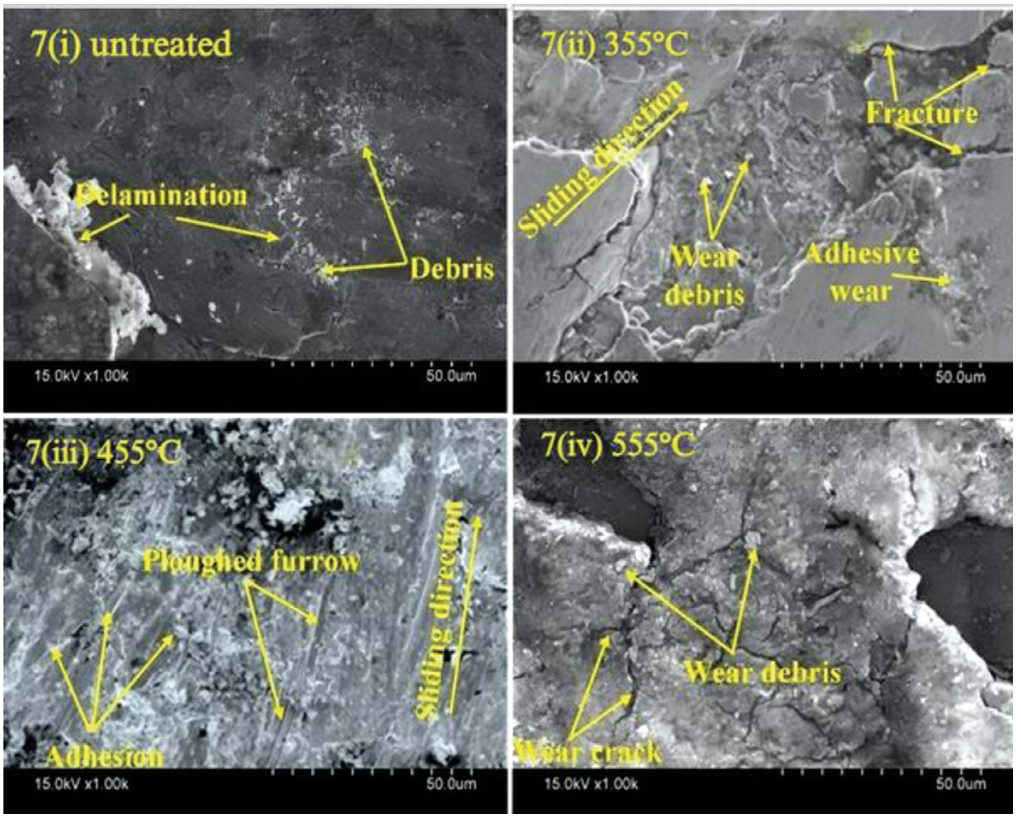

Figure 7: SEM pictures illustrating the worn surface morphologies of ENB coatings with a $NaBH_4$ concentration of 0.90 g/L in the following conditions: (i) the untreated state; after heat treatment at (ii) 355 °C; (iii) 455 °C; (iv) 555 °C

When comparing heat-treated coatings to their untreated equivalents, the average COF values tend to rise over the operational range. The compact surface topology causes a modest decrease in the COF at 455 °C. Nonetheless, the aggregate clusters that provide a grape-like surface structure at 355 and 555 °C may help to raise the average COF of the coatings made with low $NaBH_4$ concentrations. After heat treatment, the coatings made with a medium concentration of $NaBH_4$ show higher COF values, most likely as a result of their rough surface revealing clear grain boundaries. Cluster formations might also be a factor in this increase in the COF. When compared to the untreated coatings, the heat-treated ENB coatings' COF significantly increases at higher concentrations of $NaBH_4$. The surface roughness of high-$NaBH_4$ ENB coatings is naturally high and gets much rougher after heat treatment, increasing the COF. Nodule fusion and expansion can provide a texture resembling blackberries. Although this roughness should theoretically increase the COF, the surface smoothing eventually results from the compression of the asperity peaks and the filling of the roughness valleys. This smoothing effect stabilizes and sometimes reduces the COF over the temperature range for heat treatment.

Table 1 provides particular information about ENB coating wear rates. Low quantities of $NaBH_4$ in the coatings heat-treated at 455 °C show an increasing wear rate. The wear rate is still higher than that in the untreated state, notwithstanding a minor decrease at 555 °C. While rougher surfaces tend to accelerate wear, improved surface hardness often lessens it.[3] Larger nodules in low-boron coatings result in greater roughness and decreased hardness following heat treatment, which could account for the higher specific wear rate. As the heat treatment temperature rises, the wear rate decreases in the coatings that contain medium to high concentrations of $NaBH_4$. In contrast to the COF, in the untreated ENB coatings, the wear rate first rises with the concentration of $NaBH_4$.[11] Elevated $NaBH_4$concentrations have the potential to accelerate wear by breaking down surface asperities.[24] At a temperature of 555 °C, the wear rate of the coatings containing moderate to high levels of $NaBH_4$ shows a noticeable decrease. This may be attributed to the higher boron concentration and the grain structure undergoing recrystallization following heat treatment.[8] The reduction in the specific wear rate can be attributed to the enhanced surface hardness resulting from higher boron levels in the ENB coatings,[3,4] which occur as the $NaBH_4$ concentration increases.[3,4,11]

Figures 6, **7**, and **8** present SEM images highlighting the damaged regions of the ENB coatings. The observation of wear debris distributed along the wear path, as illustrated in **Figures 6i** and **8i**, indicates that adhesive wear is the prevailing mechanism in the untreated coatings. Wear grooves form along the sliding direction, in part due to repetitive sliding loads.[17,24] As seen in **Fig-**

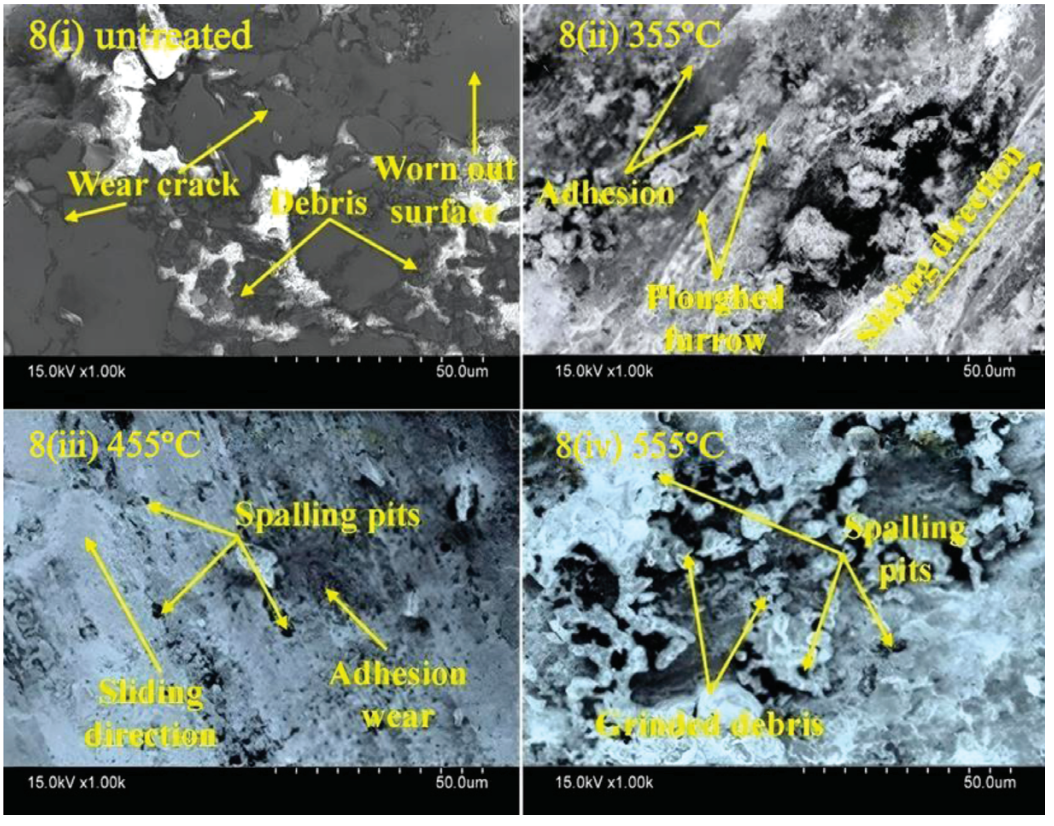

Figure 8: SEM pictures illustrating the worn surface morphologies of ENB coatings with a $NaBH_4$ concentration of 1.20 g/L in the following conditions: (i) the untreated state; after heat treatment at (ii) 355 °C; (iii) 455 °C; (iv) 555 °C

ures 6ii and **7i**, plowing effects can cause the top layer of coatings to delaminate in some areas. Heat-treated coatings, on the other hand, have a rougher surface because the asperities have been significantly fragmented and compressed. Furthermore, worn debris acts as a load-bearing zone by adhering to the sliding surface or building up along the sliding route. In these circumstances, the wear resistance increases as the heat-treatment temperature rises[8,11] and COF values may fall.[23]

In borohydride-reduced ENB coatings, adhesive wear is the predominant wear mechanism, outperforming abrasive and delamination wear. Significant mass loss happens during the first sliding phase as a result of the removal of surface roughness peaks, increasing the wear rate. But during tribological testing, some wear debris adheres to the sliding surface, forming a layer that separates it from the counter surface.[11] The particular wear rate of heat-treated coatings may be lowered as a result of this phenomenon.[8] Furthermore, in the sliding direction, spalling or pitting is visible, most likely as a result of accumulated debris and adhesive wear. Adhesive wear is thus identified as the primary and most common wear mechanism in borohydride-reduced ENB coatings, in both their untreated and heat-treated states.

SEM images and tribological data indicate that heat treatment reduces surface asperities by fusing nodules into a compact structure, which in turn decreases roughness valleys. This structural densification minimizes stress concentration points, thereby reducing the probability of crack initiation, and also providing smoother sliding conditions that lead to reduced abrasive wear. However, the influence of heat treatment is strongly temperature dependent. At 355 °C, the reduction in roughness is only partial, and the wear rate remains higher due to grain boundary weakness. At 455 °C, a significant decrease in roughness is observed, along with the formation of hard Ni_2B phases, resulting in the lowest wear rate and the highest scratch hardness. At 555 °C, although the surface roughness decreases further, the coarsening of Ni_3B phases reduces the compactness of the coating, causing a slight increase in wear.

Coatings based on electroless nickel are frequently used to modify surfaces. However, the disposal of hazardous materials employed in the coating bath makes the electroless deposition technique problematic for the environment. Some baths use $PbNO_3$, a stabilizer that has been banned in a number of countries. Cleaner production methods, including physical and chemical vapour deposition, are being investigated in response to environmental regulations. However, due to its better mechanical and tribological qualities, electroless deposition is still important despite these developments.[25,26] Alternative stabilizers like bismuth and tin are being studied as possible replacements for lead-based compounds, and researchers are striving to create lead-free baths.[27,28] Consequently, the scientific community is increasingly focusing on initiatives to make electroless coating techniques more ecologically friendly.[29] Ceramic-coated Al6061 alloys, produced by thermal plasma deposition to enhance wear resistance in engine applications, improve durability but face challenges like microcracks and porosity.[30] TiC and WC coatings applied via ESD can improve AISI 1040 steel's wear and corrosion resistance. WC coatings show superior wear resistance, while TiC provides better corrosion protection. Both coatings exhibit uniform microstructures including carbides like $M_{23}C_6$ and M_7C_3.[31] A plasma-sprayed 99 % Cr_2O_3 coating on AISI 1040 forged steel shows the highest microhardness and wear resistance due to its dense, defect-free structure and strong adhesion. Increasing the TiO_2 content reduces hardness. Coating performance correlates with microhardness. Cr_2O_3 is ideal for enhancing the wear resistance of sugar mill roll shafts.[32]

4 CONCLUSIONS

Untreated ENB coatings initially exhibit an amorphous or mixed amorphous-nanocrystalline structure that gradually transforms into a crystalline phase during operation.

A larger boron percentage causes the nanohardness to grow with $NaBH_4$ concentration.

Heat treatment enhances hardness not only through the development of a dense surface structure but also by promoting the formation of hard crystalline phases such as Ni, Ni_2B, and Ni_3B.

An increase in $NaBH_4$ concentration in the untreated state leads to a larger nodule formation, which in turn enhances the elastic modulus. Upon heat treatment, these nodules expand significantly and form cluster-like structures, contributing to a further rise in the elastic modulus.

With an increase in the $NaBH_4$ concentration, the COF in the untreated state exhibits a declining trend. However, across all temperature ranges and irrespective of the $NaBH_4$ concentration, the COF values after heat treatment remain consistently higher than those observed in the untreated coatings.

The enhanced hardness, wear resistance, and scratch durability of heat-treated Ni-B coatings underscore their strong industrial relevance, making them well-suited for critical applications in automotive and aerospace components, sugar mills and food processing equipment, mould and die tooling, as well as oil and gas equipment.

5 REFERENCES

[1] F. Bulbul, H. Altun, V. Ezirmik, O. Kucuk, Investigation of structural, tribological and corrosion properties of electroless Ni-B coating deposited on 316l stainless steel, Proceedings of the Institution of Mechanical Engineers, Part J: Journal of Engineering Tribology, 227 (**2013**), 629–639

[2] Y. Wan, Y. Yu, L. Cao, M. Zhang, J. Gao, C. Qi, Corrosion and tribological performance of PTFE-coated electroless nickel boron coatings, Surface and Coatings Technology, 307 (**2016**), 316–323

[3] M. Barman, T. K. Barman, P. Sahoo, Effect of borohydride concentration on tribological and mechanical behavior of electroless Ni-B coatings, Materials Research Express., 6 (**2019**) 12, 126575

[4] S. Surdem, C. Eseroglu, R. Citak, A parametric study on the relationship between $NaBH_4$ and tribological properties in the nickel-boron electroless depositions, Materials Research Express, 6 (**2019**) 12, 125085

[5] S. Pal, R. Sarkar, V. Jayaram, Characterization of thermal stability and high-temperature tribological behavior of electroless Ni-B coating, Metallurgical and Materials Transactions A, 49 (**2018**) 8, 3217–3236

[6] S. Pal, N. Verma, V. Jayaram, S. K. Biswas, Y. Riddle, Characterization of phase transformation behaviour and microstructural development of electroless Ni-B coating, Materials Science and Engineering: A, 528 (**2011**) 28, 8269–8276

[7] A. Mukhopadhyay, T. K. Barman, P. Sahoo, Co-deposition of W and Mo in electroless Ni-B coating and its effect on the surface morphology, structure, and tribological behavior, Proceedings of the Institution of Mechanical Engineers, Part L: Journal of Materials: Design and Applications, 235 (**2021**) 1, 49–161

[8] S. Arias, J. G. Castano, E. Correa, F. Echeverría, M. Gomez, Effect of heat treatment on tribological properties of Ni-B coatings on low carbon steel: wear maps and wear mechanisms, Journal of Tribology, 141 (**2019**) 9, 091601

[9] J. N. Balaraju, A. Priyadarshi, V. Kumar, N. T. Manikandanath, P. P. Kumar, B. Ravisankar, Hardness and wear behaviour of electroless Ni-B coatings, Materials Science and Technology, 32 (**2016**) 16, 654–665

[10] R. A. Yildiz, K. Genel, T. Gulmez, Effect of heat treatments for electroless deposited Ni-B and Ni-W-B coatings on 7075 Al alloy, International Journal of Materials, Mechanics and Manufacturing, 5 (**2017**) 2, 83–86

[11] V. Vitry, L. Bonin, Increase of boron content in electroless nickel-boron coating by modification of plating conditions, Surface and Coatings Technology, 311 (**2017**), 164–171

[12] C. Dominguez-Rios, A. Hurtado-Macias, R. Torres-Sanchez, M. A. Ramos, J. Gonzalez-Hernandez, Measurement of mechanical properties of an electroless Ni-B coating using nanoindentation, Industrial & Engineering Chemistry Research, 51 (**2012**) 22, 7762–7768

[13] M. G. Hosseini, S. Ahmadiyeh, A. Rasooli, S. Khameneh-Asl, Pulse plating of Ni-W-B coating and study of its corrosion and wear resistance, Metallurgical and Materials Transactions A, 50 (**2019**) 11, 5510–5524

[14] V. Nemane, S. Chatterjee, Scratch and sliding wear testing of electroless Ni-B-W coating, Journal of Tribology, 142 (**2020**) 2, 021705

[15] A. B. Radwan, R. A. Shakoor, A. Popelka, Improvement in properties of Ni-B coatings by the addition of mixed oxide nanoparticles, International Journal of Electrochemical Science, 10 (**2015**) 9, 7548–7562

[16] V. Niksefat, M. Ghorbani, Mechanical and electrochemical properties of ultrasonic-assisted electroless deposition of Ni-B-TiO_2 composite coatings, Journal of Alloys and Compounds, 633 (**2015**), 127–136

[17] D. Dellasega, V. Russo, A. Pezzoli, C. Conti, N. Lecis, E. Besozzi, M. Beghi, C. E. Bottani, M. Passoni, Boron films produced by high energy pulsed laser deposition, Materials & Design, 134 (**2017**), 35–43

[18] A. Mukhopadhyay, T. K. Barman, P. Sahoo, Effect of operating temperature on tribological behavior of as-plated Ni-B coating deposited by electroless method, Tribology Transactions, 61 (**2018**) 1, 41–52

[19] F. Bulbul, The effects of deposition parameters on surface morphology and crystallographic orientation of electroless Ni-B coatings, Metals and Materials International, 17 (**2011**) 1, 67–75

[20] P. Biswas, S. Samanta, A. R. Dixit, R. Sahoo, Investigation of mechanical and tribological properties of electroless Ni-P-B ternary coatings on steel, Surface Topography: Metrology and Properties, 9 (**2021**) 3, 035011

[21] J. K. Pancrecious, J. P. Deepa, V. Jayan, U. S. Bill, T. P. D. Rajan, B. C. Pai, Nanoceria induced grain refinement in electroless Ni-B-CeO_2 composite coating for enhanced wear and corrosion resistance of aluminium alloy, Surface and Coatings Technology, 356 (**2018**), 29–37

[22] S. Pal, V. Jayaram, Effect of microstructure on the hardness and dry sliding behavior of electroless Ni-B coating, Materialia, 4 (**2018**), 47–64

[23] X. Liu, Y. Fuping, W. Yueguang, Grain size effect on the hardness of nanocrystal measured by the nanosize indenter, Applied Surface Science, 279 (**2013**), 159–166

[24] F. Madah, C. Dehghanian, A. A. Amadeh, Investigations on the wear mechanisms of electroless Ni-B coating during dry sliding and endurance life of the worn surfaces, Surface and Coatings Technology, 282 (**2015**), 6–15

[25] L. Bonin, V. Vitry, F. Delaunois, Inorganic salts stabilizers effect in electroless nickel-boron plating: Stabilization mechanism and microstructure modification, Surface and Coatings Technology, 401 (**2020**), 126276

[26] M. Yunacti, A. Megret, M. H. Staia, A. Montagne, V. Vitry, Characterization of electroless nickel-boron deposit from optimized stabilizer-free bath, Coatings, 11 (**2021**) 5, 576

[27] L. Bonin, V. Vitry, F. Delaunois, The tin stabilization effect on the microstructure, corrosion and wear resistance of electroless Ni-B coatings, Surface and Coatings Technology, 357 (**2019**), 353–363

[28] L. Bonin, V. Vitry, F. Delaunois, Replacement of lead stabilizer in electroless nickel-boron baths: synthesis and characterization of coatings from bismuth stabilized bath, Sustainable Materials and Technologies, 23 (**2020**), e00130

[29] S. Banerjee, P. Sarkar, P. Sahoo, Improving corrosion resistance of magnesium nanocomposites by using electroless nickel coatings, Facta Universitatis – Series: Mechanical Engineering, 20 (**2022**), doi:10.22190/FUME210714068B

[30] C. Suresh, D. R. P. Rajarathnam, A. P. Sivasubramaniam, G. Saravanan, Investigation of the wear-resistance characteristics of alumina-zirconia-titania-coated Al-6061 alloy for different processing parameters, Mater. Tehnol., 59 (**2025**), 307–314

[31] D. R. P. Rajarathnam, K. Sundaramurthy, M. Makesh, R. Meiyazhagan, Assessment of Wear and Corrosion Resistance in TiC and WC Coatings applied to AISI 1040 Forged Steel via Electrospark Deposition, Mater. Tehnol., 59 (**2025**), 39–46

[32] D. R. P. Rajarathnam, Murugesan Jayaraman, Investigation of the wear behaviour of an AISI 1040 forged steel shaft with plasma-spray ceramic-oxide coatings for sugar-cane mills, Mater. Tehnol., 51 (**2017**), 95–100